

LETTER • OPEN ACCESS

Compound marine heatwaves and low sea surface salinity extremes over the tropical Pacific Ocean

To cite this article: Hao Liu *et al* 2023 *Environ. Res. Lett.* **18** 064001

View the [article online](#) for updates and enhancements.

You may also like

- [The record-breaking 2022 long-lasting marine heatwaves in the East China Sea](#)
Hyooun Oh, Go-Un Kim, Jung-Eun Chu et al.
- [The rapid rise of severe marine heat wave systems](#)
J Xavier Prochaska, Claudie Beaulieu and Katerina Giamalaki
- [Subseasonal prediction of the 2020 Great Barrier Reef and Coral Sea marine heatwave](#)
Jessica A Benthuisen, Grant A Smith, Claire M Spillman et al.

The Breath Biopsy® Guide
Fourth edition

FREE

DOWNLOAD THE FREE E-BOOK

BREATH BIOPSY

OWLSTONE MEDICAL

ENVIRONMENTAL RESEARCH
LETTERS

LETTER

Compound marine heatwaves and low sea surface salinity extremes over the tropical Pacific Ocean

OPEN ACCESS

RECEIVED
2 February 2023REVISED
26 April 2023ACCEPTED FOR PUBLICATION
27 April 2023PUBLISHED
10 May 2023

Original content from this work may be used under the terms of the [Creative Commons Attribution 4.0 licence](#).

Any further distribution of this work must maintain attribution to the author(s) and the title of the work, journal citation and DOI.

Hao Liu^{1,2,3,4} , Xunwei Nie^{2,3,4} , Chaoran Cui¹ and Zexun Wei^{2,3,4,*} ¹ Institute of Oceanographic Instrumentation, Qilu University of Technology (Shandong Academy of Science), Qingdao, People's Republic of China² Laboratory for Regional Oceanography and Numerical Modeling, Laoshan Laboratory, Qingdao, People's Republic of China³ First Institute of Oceanography, and Key Laboratory of Marine Science and Numerical Modeling, Ministry of Natural Resources, Qingdao, People's Republic of China⁴ Shandong Key Laboratory of Marine Science and Numerical Modeling, Qingdao, People's Republic of China

* Author to whom any correspondence should be addressed.

E-mail: weizx@fio.org.cn**Keywords:** marine heatwaves, salinity extremes, salinity budget, temperature budget, compound extreme events, ENSO**Abstract**

Marine heatwaves (MHWs) and low sea surface salinity (SSS) events can significantly impact marine ecosystems and dynamic systems, respectively. Compound marine extreme events can cause more significant damage than individual extreme events. However, the spatiotemporal patterns of compound MHW-low SSS extremes are not well understood. Daily reanalysis data were used to identify the basic patterns of compound extreme events and their drivers. These events mainly occur over the central tropical Pacific Ocean during record-breaking El Niño events. This analysis revealed that extreme sea surface warming associated with El Niño drives increased convection, which subsequently leads to increased rainfall. It ultimately causes extreme sea surface freshening. This analysis highlights the significance of air-sea interactions and low-frequency climate variability in shaping compound extreme events.

1. Introduction

Marine extreme events, such as marine heatwaves (MHWs, Hobday *et al* 2016), low-salinity extremes (Alosairi *et al* 2019, Poppeschi *et al* 2021), and ocean acidity extremes (Burger *et al* 2022) can have harmful impacts on marine ecosystems (Smale *et al* 2019 for MHWs; Li *et al* 2022 for the low-salinity state; Burger *et al* 2020 for ocean acidity extremes). However, even more of concern is the occurrences of multiple synchronized extreme events as they place greater stress on the natural systems than individual extremes (Gruber *et al* 2021).

High sea surface temperature (SST) and low sea surface salinity (SSS) can lead to increased outbreaks of epiphytic filamentous algae and tissue necrosis, resulting in the loss of the seaweed *Kappaphycus alvarezii* (Pickering *et al* 2011). Additionally, these events can also lead to intensified stratification (Fu *et al* 2016), which causes weaker vertical mixing. As a result, less nutrients are transferred from

the subsurface to the photic zone, thereby reducing primary production. Although compound MHW-low SSS extreme (SSSmin) events are important to marine biota and dynamic systems, their characteristics remain understudied.

The causes of MHWs are associated with global warming (Frölicher and Laufkötter 2018, Laufkötter *et al* 2020), and both the intensity and duration of MHWs are expected to increase in the 21st century under a warming trend (Frölicher and Laufkötter 2018). Meanwhile, the global hydrological cycle is intensified under global warming conditions (Held and Soden 2006, Xie *et al* 2010, Zhou *et al* 2011, Qian and Chen 2014), thereby driving 'wet regions to become wetter.' Over the tropical Pacific, SSS is decreasing most significantly (Durack and Wijffels 2010, Durack *et al* 2012, Skliris *et al* 2014), where tropical oceans feature a fresh band due to excessive rainfall. As global warming has persisted for the last several decades (Johnson and Lyman 2020), warmer SST and lower SSS are expected over the tropical ocean.

In this study, we focus on the tropical Pacific Ocean, where MHWs exhibit maximum intensity (Jacox *et al* 2020) and the sea surface displays strong freshening compared to the rest of global ocean (Durack and Wijffels 2010). Drivers of SST and SSS variability over the tropical ocean can be identified using the temperature budget (Marin *et al* 2022, Vogt *et al* 2022) and salinity budget (Hasson *et al* 2013, Gasparin and Roemmich 2016), respectively. Based on the temperature budget, vertical processes play a key role in sea surface heating during MHWs over the tropical Pacific Ocean (Vogt *et al* 2022). The salinity budget indicates that rainfall led to a decrease in SSS during 2015–2016 (Gasparin and Roemmich 2016). Despite a comprehensive understanding of the drivers of extreme warming (Holbrook *et al* 2019, Vogt *et al* 2022) and freshening (Gasparin and Roemmich 2016) over the tropical Pacific Ocean in specific cases, the underlying drivers of MHW-SSSmin events remain unknown. Since MHW-SSSmin events can place more severe stresses on ecosystems and dynamic systems than individual extreme events, our study aims to uncover the patterns of these events and their associated drivers.

2. Data and methods

2.1. Data

The MHWs and SSSmin were analyzed using two reanalysis datasets: daily ocean variables from the first version of the 1/12° horizontal resolution Global Ocean Reanalysis and Simulations (GLORYS12V1; reference number CMEMS-GLO-PUM-001-030) and hourly air-sea flux data from the European Center for Medium-Range Weather Forecasts Reanalysis v5 (ERA5 hereafter, Hersbach *et al* 2020).

Daily SSTs, SSSs, and other ocean variables were extracted from GLORYS12V1, which assimilates observational ocean data using an eddy-resolving ocean model. The parameters are provided on a daily time scale and cover 1993–2019. The uppermost vertical level (i.e. 0.5 m) of temperature and salinity in the model grid was used to represent SST and SSS.

Precipitation, evaporation, heat fluxes, and other atmospheric variables were derived from ERA5 (Hersbach *et al* 2020). Hourly ERA5 data were collected and converted to daily data. The ERA5 data cover 1959 to the present. The horizontal resolution was 0.25°.

2.2. Methods

All datasets were interpolated to 1° × 1°, except for those that were used for the calculation of horizontal advection. The longest common period extended from 1993 to 2019, which is the temporal coverage in this analysis. Practical salinity was converted to absolute salinity (McDougall and Barker 2011) in this analysis.

2.2.1. Definition of extreme and compound events

In accordance with Hobday *et al* (2016), an MHW is defined as an event where the daily SST exceeds the 90th percentile threshold for each calendar day. Similarly, a SSSmin occurs when the SSS anomalies are below the 10th percentile. When MHW and SSSmin events occur concurrently in time and space, they are known as compound events. The likelihood multiplication factor (LMF, Grix *et al* 2021) is used to quantify the ratio between the observed likelihood of the compound event and the product of the individual likelihoods of the extreme events. LMF is written as

$$LMF = \frac{p(MHW - SSSmin)}{p(MHW) \times p(SSSmin)} \quad (1)$$

where $p(MHW - SSSmin)$ denotes the likelihood of compound events and $p(MHW)$ and $p(SSSmin)$ denote the likelihoods of MHWs and SSSmin, respectively. p is derived from the ratio of the total number of extreme days to the length of the study period. An LMF above 1 indicates that compound events occur more frequently than by chance, and an LMF below 1 indicates that the two events occur independently, and the likelihood of a compound event is small.

2.2.2. Budget analysis

To explore the relative contributions of different physical processes to compound MHW-SSSmin events, mixed-layer heat and salinity budget analyses were performed (Huang *et al* 2010, Vijith *et al* 2020). Mixed layer salinity (MLS) and temperature (MLT) are defined as the vertically averaged salinity and temperature between the sea surface and the bottom of the mixed layer, which can represent the variations in SSS and SST (Huang *et al* 2010). Vijith *et al* (2020) derived a closed mixed layer heat budget equation based on observations. In this study, the reanalysis data do not provide vertical velocity, vertical eddy diffusivity, or horizontal eddy diffusivity. Therefore, we have combined these terms in the residuals, which also includes the computational error. The modified budget equations are as follows:

$$\underbrace{\frac{\partial T_a}{\partial t}}_{Temp\ Tend} = - \underbrace{\left[u_a \frac{\partial T_a}{\partial x} + v_a \frac{\partial T_a}{\partial y} \right]}_{ADV} - \underbrace{\left[\frac{T_a - T_{-h}}{h} \right] \left[\frac{\partial h}{\partial t} + u_{-h} \frac{\partial h}{\partial x} + v_{-h} \frac{\partial h}{\partial y} \right]}_{ENT} + \underbrace{\frac{Q_{net} - Q_{pen}}{h \rho_0 c_p}}_{HFlux} + Residual \quad (2)$$

$$\begin{aligned}
 \underbrace{\frac{\partial S_a}{\partial t}}_{\text{Salt Tend}} = & - \underbrace{\left[u_a \frac{\partial S_a}{\partial x} + v_a \frac{\partial S_a}{\partial y} \right]}_{\text{ADV}} \\
 & - \underbrace{\left[\frac{S_a - S_{-h}}{h} \right] \left[\frac{\partial h}{\partial t} + u_{-h} \frac{\partial h}{\partial x} + v_{-h} \frac{\partial h}{\partial y} \right]}_{\text{ENT}} \\
 & + \underbrace{\frac{S_a}{h} (E - P)}_{\text{FWF}} + \text{Residual} \quad (3)
 \end{aligned}$$

where subscript a denotes the variable vertically averaged between the sea surface and the bottom of the mixed layer, and subscript $-h$ denotes the quantity at the bottom of the mixed layer. T is the temperature, S is the salinity, and h is the mixed layer depth (MLD), which is defined based on a 0.03 kg m^{-3} density threshold (de Boyer Montégut *et al* 2004). u and v are horizontal velocities. Q_{net} is the net heat flux, and Q_{pen} is the shortwave radiation penetrating through the bottom of the MLD. Q_{net} and Q_{pen} were derived using the same procedures in Huang *et al* (2010). E and P are evaporation and precipitation, respectively. ρ_0 denotes the reference density (1025 kg m^{-3}), and c_p denotes the heat capacity of seawater ($3850 \text{ J kg}^{-1} \text{ }^\circ\text{C}^{-1}$).

The left-hand sides of equations (2) and (3) denote the temperature tendency (Temp Tend) and the salinity tendency (Salt Tend), respectively. The first set of terms on the right-hand side (in parentheses) in equations (2) and (3) denotes horizontal advection (ADV), the second set of terms denotes entrainment (ENT), and the third set denotes air-sea surface fluxes (HFlux for heat fluxes and FWF for freshwater fluxes). The last term denotes the residual, which is the difference between Tend and the sum of ADV, ENT and air-sea fluxes.

3. Results

3.1. Pattern of compound MHW-SSSmin events

The maximum likelihoods of MHWs (>0.09 , figure 1(a)) are observed over the central tropical Pacific Ocean. This likelihood distribution extends towards the poleward flanks of the eastern tropical ocean. In contrast, the western Pacific displays lower likelihoods of MHWs, with magnitudes below 0.07. This distribution is similar to the spatial distribution of the annual mean MHW duration (duration is defined as the time between start and end dates), which display its maximum values from the central to the eastern tropical Pacific and lower values elsewhere (Pilo *et al* 2019, Hayashida *et al* 2020). The minimum likelihoods of SSSmin (<0.08) are mostly located below the Intertropical Convergence Zone (ITCZ, Byrne *et al* 2018), with high likelihoods observed in

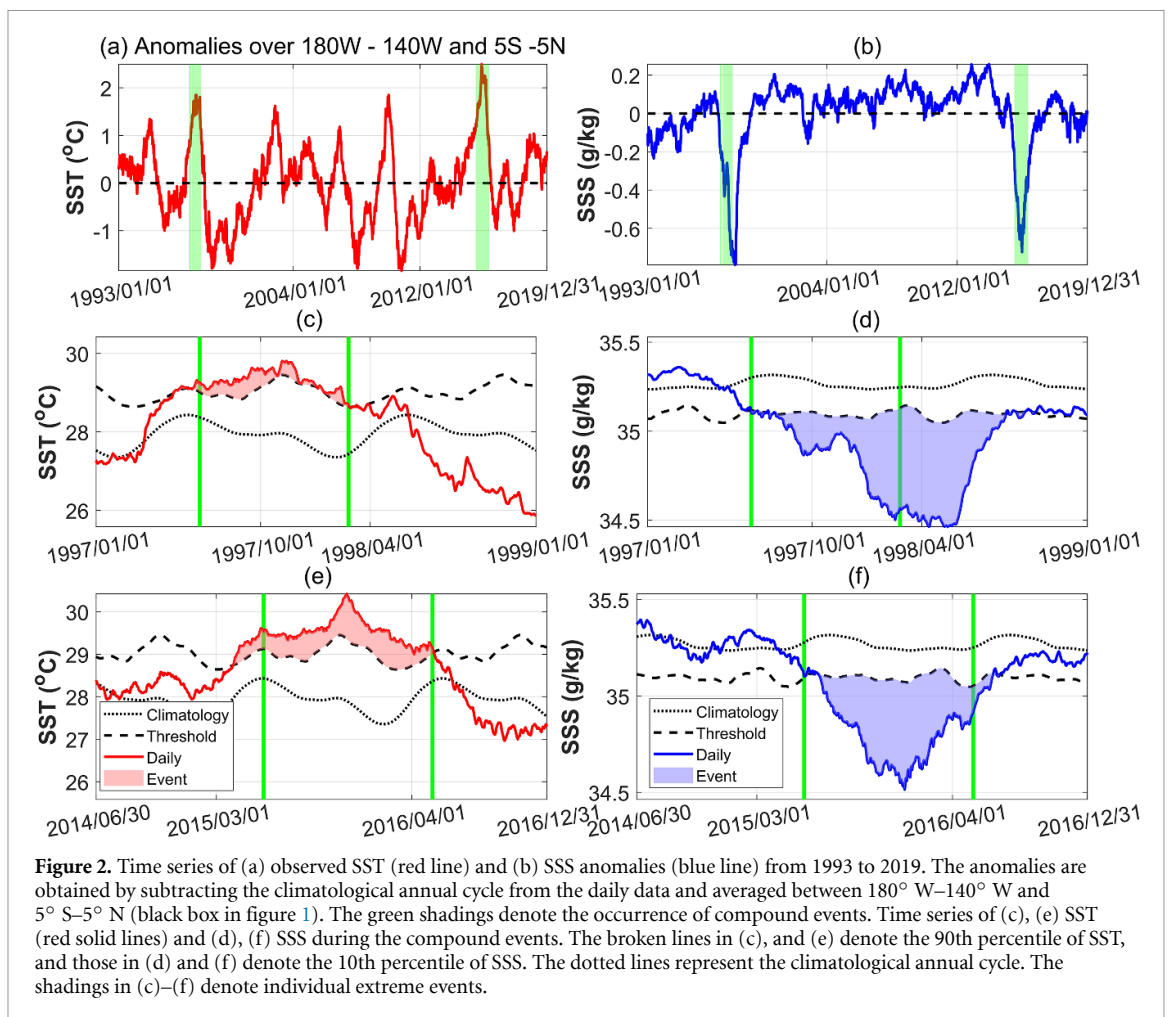
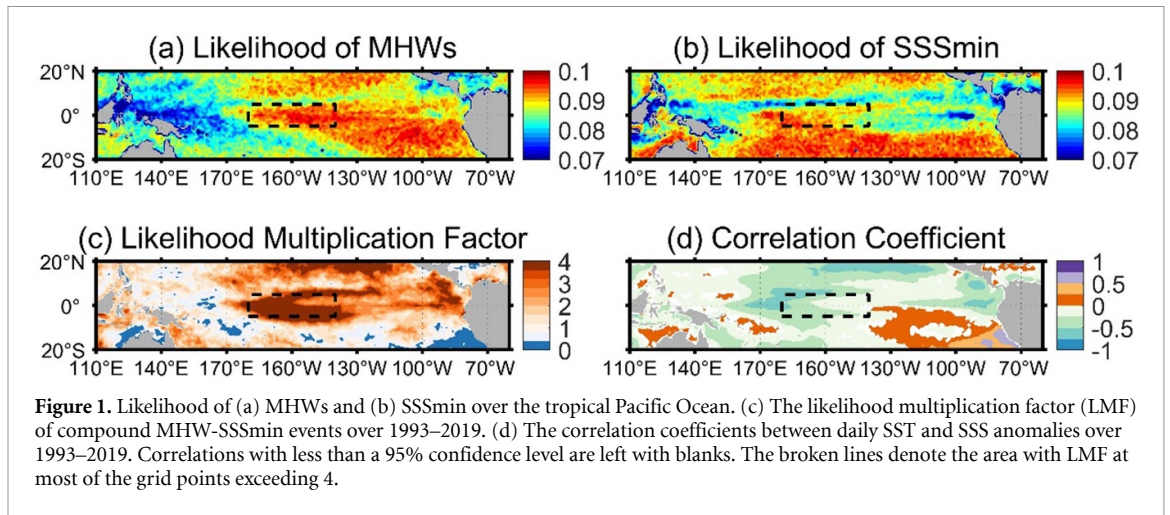
the central tropical and subtropical Pacific (>0.09 , figure 1(b)). As the SSS exhibits stronger variability (Liu and Wei 2021) under the ITCZ, the increased variability may reduce the persistence time of individual SSSmin events, leading to a lesser number of total extreme days.

Compound MHW-SSSmin extremes were most frequent in the central tropical Pacific Ocean (between 180° W – 140° W and 5° S – 5° N), where both the likelihoods of MHWs and SSSmin are large. This is four times more frequent ($\text{LFM} > 4$) than expected if SST and SSS variations were assumed to be independent. In the eastern equatorial Pacific Ocean (east of 140° W), compound events are less frequent over most of the grid points than those in the central Pacific Ocean, but the LMF is still larger than 1. In the western Pacific warm pools, compound events were the least frequent, occurring in less than 1% of the days.

Hotspots of compound events occurred where SST and SSS anomalies were negatively correlated (with a magnitude of 0.07–0.57, above the 95% confidence level, figure 1(d)). Positive correlation coefficients (with a magnitude of 0.15–0.6, above the 95% confidence level) were found where a low LMF occurred. Thus, over most of the tropical Pacific Ocean, the correlation coefficient is a good indicator of the LMF. Burger *et al* (2022) showed that if the components of compound events both satisfy the normal distribution, the correlation coefficient can determine the LMF. However, in our cases, we cannot make such an assumption because one prominent discrepancy existed over the northwestern side of the black box ($\text{LMF} > 4$), where strong correlation coefficients were collocated with a relatively smaller LMF (0–2). This suggests that the dependence between MHWs and SSSmin differs from the dependence in the normal distribution.

The temporal patterns, averaged between 180° W – 140° W and 5° S – 5° N (figure 2), show compound event clustering over two periods: 26 June 1997, to 24 February 1998, and 5 June 2015, to 13 May 2016. The two periods (figures 2(a) and (b)) correspond to two eastern El Niño extremes on record (Santoso *et al* 2017). SST anomalies during these events are approximately 2° C , which is associated with ENSO (Sen Gupta *et al* 2020). Simultaneously, SSS anomalies are between -0.7 and -0.8 g kg^{-1} , exhibiting two troughs from 1993 to 2019. The large salinity anomalies near the dateline are also associated with eastern El Niño (Singh *et al* 2011).

By zooming in on two compound events (figures 2(c)–(f)), we found that the onset and peak of MHWs occurred before the onset and peak (the maximum magnitude of SSS anomalies) of SSSmin events, respectively. During 1997–1998, the onset (peak) of MHWs occurred on 6 June 1997



(12 November 1997), whereas the onset (peak) of SSSmin occurred on 26 June 1997 (8 May 1998). During 2015–2016, the onset (peak) of MHWs occurred on 4 April 2015 (19 November 2015), whereas the onset (peak) of SSSmin occurred on 5 June 2015 (26 December 2015). Thus, MHWs occurred at least 20 days before the occurrence of SSSmin.

3.2. Potential drivers of MHW-SSSmin events

To better understand the dependence between MHWs and SSSmin, the underlying drivers were quantified by calculating the MLT and MLS budget averaged between 180° W–140° W and 5° S–5° N (figure 3). Figures 3(a) and (b) show that advection and entrainment provided positive anomalies and

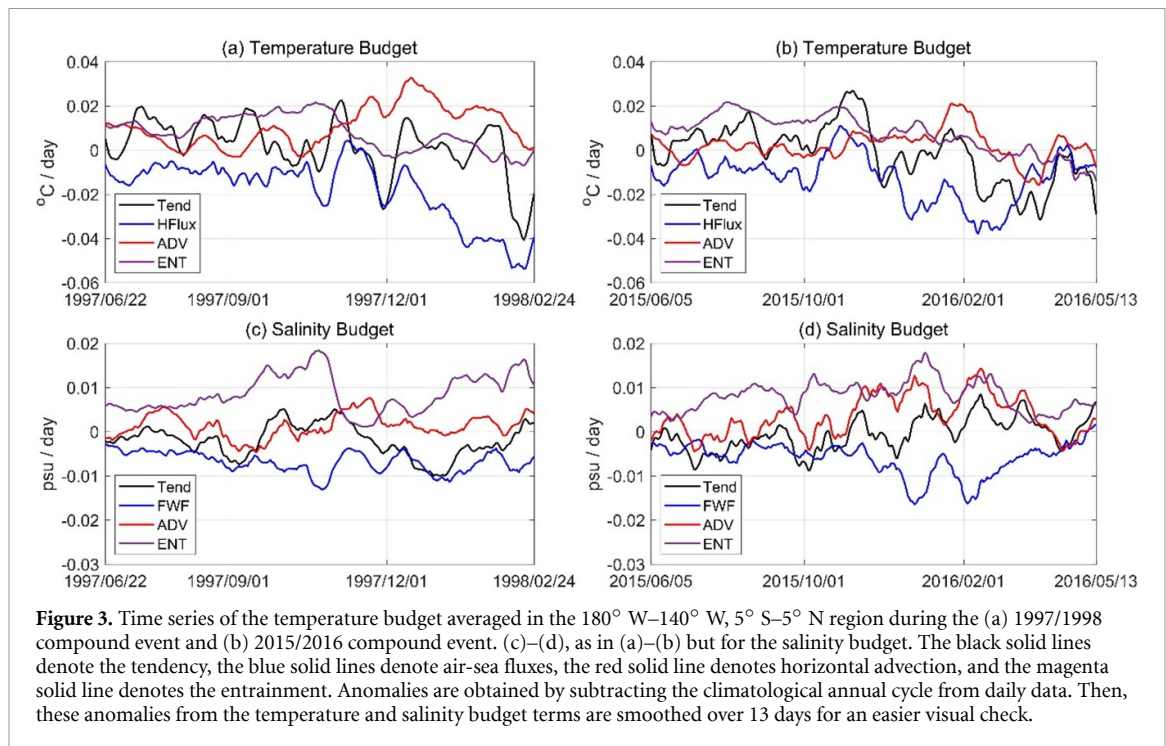


Figure 3. Time series of the temperature budget averaged in the 180° W– 140° W, 5° S– 5° N region during the (a) 1997/1998 compound event and (b) 2015/2016 compound event. (c)–(d), as in (a)–(b) but for the salinity budget. The black solid lines denote the tendency, the blue solid lines denote air-sea fluxes, the red solid line denotes horizontal advection, and the magenta solid line denotes the entrainment. Anomalies are obtained by subtracting the climatological annual cycle from daily data. Then, these anomalies from the temperature and salinity budget terms are smoothed over 13 days for an easier visual check.

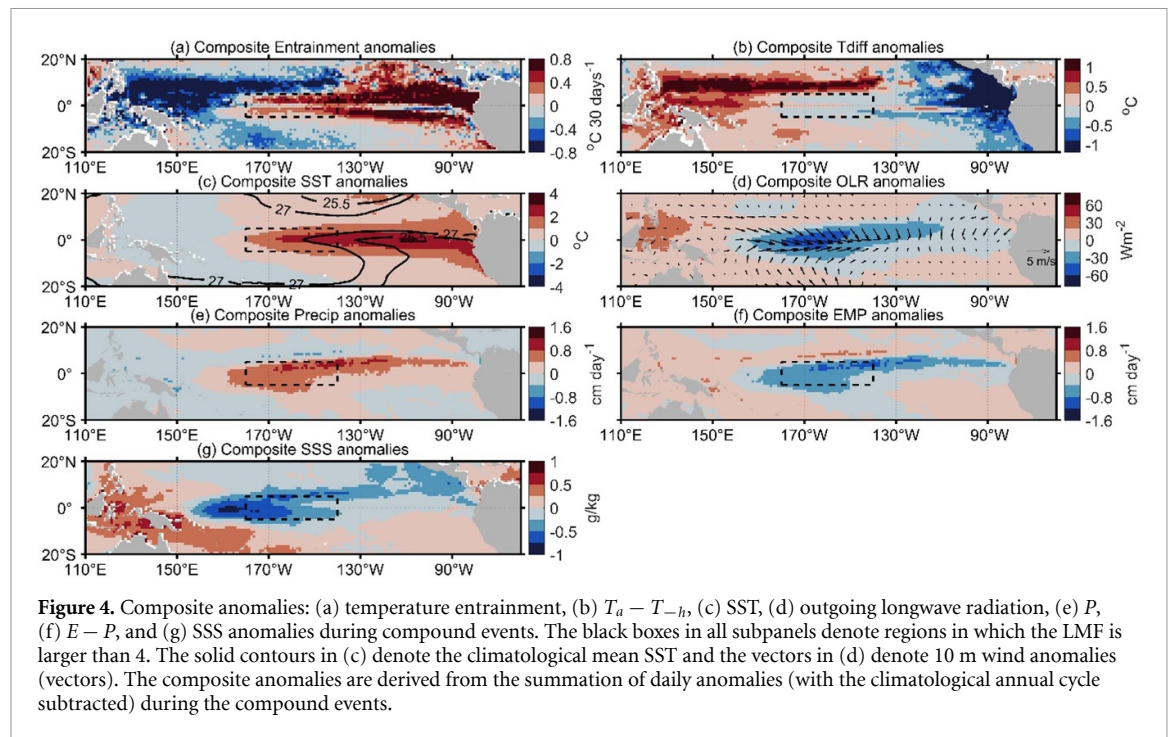
major contributions to sea surface heating during compound events. We counted the number of days in which the magnitude of ENT was stronger than that of ADV and identified that over 65% of the time, ENT played a stronger role. Thus, ENT is the key contributor to the maintenance of large SST anomalies during compound events. The results agree with those obtained for the 75 day low-pass filtered MLT terms from Huang *et al* (2011), where it was shown that subsurface processes are more important to SST variations than advection during the mature phase of ENSO.

During compound events, the ADV and surface freshwater flux (FWF) contribute to the maintenance of surface freshening. However, ADV is sometimes positive during the first 4–5 months of compound events, and FWF shows persistent negative values (figures 3(c) and (d)) during compound events. Thus, FWF plays a key role in freshening the sea surface. The results here agree with those of Gasparin and Roemmich (2016), who showed that strong precipitation in 2015 could directly cause decreases in salinity. These freshwater anomalies can also drive positive steric height anomalies in the western Pacific and increase eastward acceleration owing to the zonal pressure gradient, which leads to zonal advection.

To better understand the regional differences (figure 1(c)) and drivers (figure 3) for the occurrence of MHW-SSSmin, the anomalous signature of each variable (with the climatological annual cycle subtracted) involved during the compound events for the period 1993–2019 was analyzed (figure 4). The

anomalous temperature ENT (figure 4(a)) shows a consistent pattern with those of the SST anomalies (figure 4(c)), agreeing with the dominance of ENT during the compound events (figures 3(a) and (b)). The difference between the MLT and the temperature at a depth of 20 m below the mixed layer shows a similar pattern (figure 4(b)), but with the opposite sign (equation (2)) to ENT (due to the negative sign in front of the ENT term). This pattern is consistent with the thermocline feedback theory (Jin and An 1999), which states that mean upwelling and anomalous subsurface temperatures cause sea surface heating.

Warming over the tropical Pacific Ocean can trigger convection (characterized by outgoing long-wave radiation, OLR, Gadgil *et al* 1984, Lau *et al* 1997) when SST is above a threshold of 25.5 or 27 (figure 4(c), Lau *et al* 1997, Xie *et al* 2020). An increase in SST also leads to the convergence of winds at low altitudes (denoted by the wind speed at a height of 10 m, figure 4(d)), resulting in an intensification of convection (Xie *et al* 2020). The spatial pattern of positive SST anomalies led to a decrease in OLR, indicating an increase in convection over the central Pacific Ocean (figure 4(d)). In addition, the anomalous temperature gradient (figure 4(c)) leads to low-level wind convergence between 170° E– 130° W and 5° S– 5° N, which also implies enhanced convection. Intensified convection implies an increase in rainfall (figure 4(e)) in the central Pacific Ocean. Precipitation played the main role in the FWF ($E - P$, figure 4(f)), and the latter caused a decrease in SSS. Thus, SSS anomalies



had minimum values over the central tropical Pacific Ocean between 170°E – 130°W and 5°S – 5°N (figure 4(g)). The maximum SST anomalies ($>2^\circ\text{C}$) and minimum SSS anomalies ($<-0.5\text{ g kg}^{-1}$) are collocated at the grid points with the most frequent occurrence of MHW–SSSmin compound events.

4. Summary and discussion

MHWs and low salinity events are important for ecosystems (e.g. Smale *et al* 2019, Li *et al* 2022). However, the characteristics and drivers of compound MHW–SSSmin extremes have not been identified. In this study, we found that the hotspot of compound MHW–SSSmin mainly occurred over the central tropical Pacific Ocean (between 180°W – 140°W and 5°S – 5°N). The MLT and MLS budget show that thermohaline feedback ($T_a - T_{-h}$) plays the most important role in warming during compound events, and that FWF drives sea surface freshening. The onset and peak of SST anomalies in MHW–SSSmin events occurred before (at least 20 days) the onset and peak of SSS anomalies (figure 2). The associated mechanism might occur in the following order: (1) Subsurface temperature anomalies leading to persistent surface heating. (2) Positive SST anomalies drive convection in the central tropical Pacific Ocean. (3) Increases in rainfall are the main contributors to decreases in EMP, which leads to a decrease in SSS.

Hayashida *et al* (2020) have shown that the annual MHW days (the number of MHW days per year) show maximum values (>35 days) in the central and eastern tropical Pacific over the global ocean. This is consistent with the spatial distribution of the likelihoods of MHWs (figure 1(a)). SSSmin events

(synoptic events) are mostly studied in the vicinity of coastal/bay regions of the ocean (Alosairi *et al* 2019, Poppeschi *et al* 2021). To our knowledge, the spatial distribution of SSSmin properties has not been investigated in the tropical Pacific Ocean. Our results show that SSSmin has a maximum likelihood over the central tropical Pacific and a minimum likelihood under the ITCZ. We suspect that the high SSS variability under the ITCZ (Liu and Wei 2021) may reduce the number of days with persistent low salinity anomalies.

Previous studies have shown that the SSS front between fresh western water and salty central water migrates zonally on seasonal and interannual time scales (Qu *et al* 2014). Its correlation with the Southern Oscillation Index is -0.84 , indicating the possible role of ENSO in determining the variability of the SSS front and SSS anomalies. The results from Zhi *et al* (2021) confirmed that during El Niño, the center of negative SSS anomalies appears near the dateline. During the eastern Pacific (EP) El Niño, EP SST warming reduces the tropical Pacific SST gradient, resulting in a weakened Walker circulation (Park *et al* 2022). This leads to maximum rainfall anomalies anchored in the central tropical Pacific Ocean (Power *et al* 2013, Zhong *et al* 2019, Yan *et al* 2020). FWFs drive the SSS tendency, resulting in minimum SSS anomalies ($<-0.2\text{ psu}$, Zhi *et al* 2020) over the central Pacific Ocean. In our study, we link the EP SST warming to sea surface freshening ($<-0.5\text{ g kg}^{-1}$) based on daily reanalysis data (figure 4), and we find that the overlapping regions between the minimum SSS anomalies ($<-0.5\text{ g kg}^{-1}$) and the maximum SST anomalies ($>2^\circ\text{C}$) are where MHW–SSSmin occurs (figure 1(c)).

Sen Gupta *et al* (2020) showed that the longest and strongest MHWs in the central tropical Pacific occur during the strongest El Niños. Holbrook *et al* (2019) analyzed MHW occurrences during different climate modes and found that they are mostly linked to ENSO. In line with these findings, our study shows that the spatial pattern of SST anomalies during compound events (figure 4(a)) resemble those found during EP El Niños (figure 1 from Zhi *et al* 2021). Furthermore, we also find that MHW-SSSmin events from 1993 to 2019 were mainly observed during the two strongest eastern El Niños on record (97–98 and 15–16, figure 2). This suggests that MHW-SSSmin events are associated with EP El Niños, emphasizing the importance of low-frequency climate variability (i.e. El Niño) in compound extremes.

A caveat of this study is the neglect of vertical velocities in the SST entrainment term and the neglect of the vertical temperature diffusion term in the temperature budget calculation. We have calculated the vertical velocity based on equation of volume continuity. Results suggest that the differences in entrainment term between the two scenarios (i.e. with or without vertical velocity) are negligible (figure not shown here). Huang *et al* (2011) found that entrainment and vertical diffusion play the most important role in SST anomalies during the mature phase of El Niño. Zhang and Gao (2015) found that the subsurface entrained temperature plays a dominant role in controlling SST variability. This analysis has pointed out the important role of subsurface temperature anomalies (in entrainment) in setting SST extremes, but we cannot exclude the possible role of vertical diffusion. Therefore, additional analyses accounting for vertical diffusion processes will be performed during compound events when diffusivity data is available.

El Niño may also cause other compound extreme events, such as MHW-low chlorophyll (Le Grix *et al* 2021) extreme events. Multiple extreme events may occur simultaneously in time and space, leading to further damage to marine organisms and ecosystems. A positive consideration is that the ENSO state at forecast initialization can enhance MHWs' forecasting skill (Jacox *et al* 2022). This will enable us to improve forecasting capabilities for compound extremes and assess risks before they occur over the tropical Pacific Ocean (Zscheischler and Seneviratne 2017).

Data availability statement

The daily GLORYS12V1 was collected from <https://resources.marine.copernicus.eu/products>, and the reference number was MULTIOBS_GLO_PHY_S_SURFACE_MYNRT_015_013 for access. ERA5 hourly data were obtained from <https://cds.climate.copernicus.eu/cdsapp#!/dataset/reanalysis-era5-single-levels?tab=form>.

All data that support the findings of this study are included within the article (and any supplementary files).

Acknowledgments

Hao Liu was supported by the National Natural Science Foundation of China (No. 42006005), Chaoran Cui was supported by the Natural Science Foundation of Shandong Province (No. ZR2021QD081) and Zexun Wei was supported by the Laoshan Laboratory (No. LSKJ202202700).

Conflict of interest

The authors declare no conflicts of interest. The funders had no role in the design of the study; in the collection, analysis, or interpretation of data; or in the writing of the manuscript or in the decision to publish the results.

ORCID iDs

Hao Liu  <https://orcid.org/0000-0001-9999-5965>

Xunwei Nie  <https://orcid.org/0000-0002-4084-8335>

Zexun Wei  <https://orcid.org/0000-0002-1217-6973>

References

- Alosairi Y, Alsulaiman N, Petrov P and Karam Q 2019 Responses of salinity and chlorophyll-a to extreme rainfall events in the northwest Arabian Gulf: emphasis on Shatt Al-Arab Mar. *Pollut. Bull.* **149** 110564
- Burger F A, John J G and Frölicher T L 2020 Increase in ocean acidity variability and extremes under increasing atmospheric CO₂ *Biogeosciences* **17** 4633–62
- Burger F A, Terhaar J and Frölicher T L 2022 Compound marine heatwaves and ocean acidity extremes *Nat. Commun.* **13** 4722
- Byrne M P, Pendergrass A G, Rapp A D and Wodzicki K R 2018 Response of the intertropical convergence zone to climate change: location, width, and strength *Curr. Clim. Change Rep.* **4** 355–70
- de Boyer Montégut C, Madec G, Fischer A S, Lazar A and Iudicone D 2004 Mixed layer depth over the global ocean: an examination of profile data and a profile-based climatology *J. Geophys. Res.* **109** C12003
- Durack P J and Wijffels S E 2010 Fifty-year trends in global ocean salinities and their relationship to broad-scale warming *J. Clim.* **23** 4342–62
- Durack P J, Wijffels S E and Matear R J 2012 Ocean salinities reveal strong global water cycle intensification during 1950–2000 *Science* **336** 455–8
- Frölicher T L and Laufkötter C 2018 Emerging risks from marine heat waves *Nat. Commun.* **9** 650
- Fu W, Randerson J T and Moore J K 2016 Climate change impacts on net primary production (NPP) and export production (EP) regulated by increasing stratification and phytoplankton community structure in the CMIP5 models *Biogeosciences* **13** 5151–70
- Gadgil S, Joseph P V and Joshi N V 1984 Ocean–atmosphere coupling over monsoon regions *Nature* **312** 141–3
- Gasparin F and Roemmich D 2016 The strong freshwater anomaly during the onset of the 2015/2016 El Niño *Geophys. Res. Lett.* **43** 6452–60

- Gruber N, Boyd P W, Frölicher T L and Vogt M 2021 Biogeochemical extremes and compound events in the ocean *Nature* **600** 395–407
- Hasson A E A, Delcroix T and Dussin R 2013 An assessment of the mixed layer salinity budget in the tropical Pacific Ocean. Observations and modelling (1990–2009) *Ocean Dyn.* **63** 179–94
- Hayashida H, Matear R J, Strutton P G and Zhang X 2020 Insights into projected changes in marine heatwaves from a high-resolution ocean circulation model *Nat. Commun.* **11** 4352
- Held I M and Soden B J 2006 Robust responses of the hydrological cycle to global warming *J. Clim.* **19** 5686–99
- Hersbach H, Bell B, Berrisford P, Hirahara S, Horányi A, Muñoz-Sabater J and Thépaut J N 2020 The ERA5 global reanalysis *Q. J. R. Meteorol. Soc.* **146** 1999–2049
- Hobday A J, Alexander L V, Perkins S E, Smale D A, Straub S C, Oliver E C J and Wernberg T 2016 A hierarchical approach to defining marine heatwaves *Prog. Oceanogr.* **141** 227–38
- Holbrook N J, Scannell H A, Sen Gupta A, Benthuisen J A, Feng M, Oliver E C J and Wernberg T 2019 A global assessment of marine heatwaves and their drivers *Nat. Commun.* **10** 2624
- Huang B, Xue Y, Wang H, Wang W and Kumar A 2011 Mixed layer heat budget of the El Niño in NCEP climate forecast system *Clim. Dyn.* **39** 365–81
- Huang B, Xue Y, Zhang D, Kumar A and McPhaden M J 2010 The NCEP GODAS ocean analysis of the tropical Pacific mixed layer heat budget on seasonal to interannual time scales *J. Clim.* **23** 4901–25
- Jacox M G, Alexander M A, Amaya D, Becker E, Bograd S J, Brodie S, Hazen E L, Pozo Buil M and Tommasi D 2022 Global seasonal forecasts of marine heatwaves *Nature* **604** 486–90
- Jacox M G, Alexander M A, Bograd S J and Scott J D 2020 Thermal displacement by marine heatwaves *Nature* **584** 82–86
- Jin F-F and An S-I 1999 Thermocline and zonal advective feedbacks within the equatorial ocean recharge oscillator model for ENSO *Geophys. Res. Lett.* **26** 2989–92
- Johnson G C and Lyman J M 2020 Warming trends increasingly dominate global ocean *Nat. Clim. Change* **10** 757–61
- Lau K-M, Wu H-T and Bony S 1997 The role of large-scale atmospheric circulation in the relationship between tropical convection and sea surface temperature *J. Clim.* **10** 381–92
- Laufkötter C, Zscheischler J and Frölicher T L 2020 High-impact marine heatwaves attributable to human-induced global warming *Science* **369** 1621–5
- Le Grix N, Zscheischler J, Laufkötter C, Rousseaux C S and Frölicher T L 2021 Compound high-temperature and low-chlorophyll extremes in the ocean over the satellite period *Biogeosciences* **18** 2119–37
- Li X, Yang B, Shi C, Wang H, Yu R, Li Q and Liu S 2022 Synergistic interaction of low salinity stress with vibrio infection causes mass mortalities in the oyster by inducing host microflora imbalance and immune dysregulation *Front. Immunol.* **13** 859975
- Liu H and Wei Z 2021 Intercomparison of global sea surface salinity from multiple datasets over 2011–2018 *Remote Sens.* **13** 811
- Marin M, Feng M, Bindoff N L and Phillips H E 2022 Local drivers of extreme upper ocean marine heatwaves assessed using a global ocean circulation model *Front. Clim.* **4** 74
- McDougall T J, P M Barker 2011 Getting started with TEOS-10 and the gibbs seawater (GSW) Oceanographic toolbox (available at: www.TEOS-10.org:SCOR/IAPSOWG127)
- Park I-H, Yeh S-W, Min S-K, Ham Y-G and Kirtman B P 2022 Present-day warm pool constrains future tropical precipitation *Commun. Earth Environ.* **3** 310
- Pickering T D, Ponia B, Hair C A, Southgate P C, Poloczanska E S, Patrona L D and Silva S D 2011 *Vulnerability of Aquaculture in the Tropical Pacific to Climate Change* (Noumea: Secretariat of the Pacific Community)
- Pilo G S, Holbrook N J, Kiss A E and Hogg A M 2019 Sensitivity of marine heatwave metrics to ocean model resolution *Geophys. Res. Lett.* **46** 14604–12
- Poppeschi C, Charria G, Goberville E, Rimmelin-Maury P, Barrier N, Petton S and Tréguer P 2021 Unraveling salinity extreme events in coastal environments: a winter focus on the bay of brest *Front. Mar. Sci.* **8** 705403
- Power S, Delage F, Chung C, Kociuba G and Keay K 2013 Robust twenty-first-century projections of El Niño and related precipitation variability *Nature* **502** 541–5
- Qian C and Chen G 2014 Warmer-get-wetter or wet-get-wetter? A criterion to classify future oceanic precipitation *J. Ocean Univ. China* **13** 552–60
- Qu T, Song Y T and Maes C 2014 Sea surface salinity and barrier layer variability in the equatorial Pacific as seen from Aquarius and Argo *J. Geophys. Res.* **119** 15–29
- Santoso A, McPhaden M J and Cai W 2017 The defining characteristics of ENSO extremes and the strong 2015/2016 El Niño *Rev. Geophys.* **55** 1079–129
- Sen Gupta A, Thomsen M, Benthuisen J A, Hobday A J, Oliver E, Alexander L V and Smale D A 2020 Drivers and impacts of the most extreme marine heatwaves events *Sci. Rep.* **10** 19359
- Singh A, Delcroix T and Cravatte S 2011 Contrasting the flavors of El Niño-Southern Oscillation using sea surface salinity observations *J. Geophys. Res.* **116** C06016
- Skliris N, Marsh R, Josey S A, Good S A, Liu C and Allan R P 2014 Salinity changes in the World Ocean since 1950 in relation to changing surface freshwater fluxes *Clim. Dyn.* **43** 709–36
- Smale D A, Wernberg T, Oliver E C J, Thomsen M, Harvey B P, Straub S C and Moore P J 2019 Marine heatwaves threaten global biodiversity and the provision of ecosystem services *Nat. Clim. Change* **9** 306–12
- Vijith V, Vinayachandran P, Webber B G, Matthews A J, George J V, Kannaujia V K and Amol P 2020 Closing the sea surface mixed layer temperature budget from *in situ* observations alone: operation Advection during BoBBLE *Sci. Rep.* **10** 1–12
- Vogt L, Burger F A, Griffies S M and Frölicher T L 2022 Local drivers of marine heatwaves: a global analysis with an earth system model *Front. Clim.* **4** 847995
- Xie R, Mu M and Fang X 2020 New indices for better understanding ENSO by incorporating convection sensitivity to sea surface temperature *J. Clim.* **33** 7045–61
- Xie S-P, Deser C, Vecchi G A, Ma J, Teng H and Wittenberg A T 2010 Global warming pattern formation: sea surface temperature and rainfall *J. Clim.* **23** 966–86
- Yan Z, Wu B, Li T, Collins M, Clark R, Zhou T and Tan G 2020 Eastward shift and extension of ENSO-induced tropical precipitation anomalies under global warming *Sci. Adv.* **6** eaax4177
- Zhang R-H and Gao C 2015 Role of subsurface entrainment temperature (T_e) in the onset of El Niño events, as represented in an intermediate coupled model *Clim. Dyn.* **46** 1417–35
- Zhi H, Lin P, Fang Z, Liu H, Zhang R-H and Bai W 2021 Sea surface salinity-derived indexes for distinguishing two types of El Niño events in the tropical Pacific *Sci. China Earth Sci.* **64** 1267–84
- Zhi H, Zhang R-H, Lin P, Yu P, Zhou G and Shi S 2020 Interannual salinity variability associated with the central Pacific and Eastern Pacific El Niños in the Tropical Pacific *J. Geophys. Res.* **125** e2020JC016090
- Zhong W, Cai W, Zheng X-T and Yang S 2019 Unusual anomaly pattern of the 2015/2016 extreme El Niño Induced by the 2014 warm condition *Geophys. Res. Lett.* **46** 14772–81
- Zhou Y, Xu K M, Sud Y and Betts A 2011 Recent trends of the tropical hydrological cycle inferred from global precipitation climatology project and international satellite cloud climatology project data *J. Geophys. Res.* **116** D09101
- Zscheischler J and Seneviratne S I 2017 Dependence of drivers affects risks associated with compound events *Sci. Adv.* **3** e1700263